Exploration Geophysics (2000) ***31****, 115-125*

Modelling the airborne electromagnetic response of a vertical contact

David Annetts[1] **Fred Sugeng**[2] **James Macnae**[3] **Art Raiche**[4]

Key Words: Airborne electromagnetics, conductivity contrast, numerical modelling

ABSTRACT

Airborne electromagnetic (AEM) surveying is an important exploration tool because it can map conductivity variations over large areas at a fraction of the cost of ground survey methods. Using rapid but approximate techniques, large volumes of data may be processed to show the variation of conductivity with depth beneath the survey. These approximate methods work well in regions with horizontal layering, but in certain circumstances they can imply the presence of false conductors in the vicinity of 2D and 3D structures. By comparing the AEM response of several 2.5D models, each of which contains a lateral conductivity contrast, we show that artefacts associated with conductivity contrasts can imply the presence of a false conductor when flight direction is towards the area of greater conductivity. When flight direction was away from the area of greater conductivity artefacts associated with the lateral conductivity contrast implied a false resistor. These artefacts were of sufficiently high magnitude that they masked the response of a genuine conductor (1.0 Ω.m) at a depth of 50 m. We show that multiple-component data sets utilising the inherent directional dependence qualities of AEM prospecting systems can be used to minimise interpretational errors in the presence of lateral conductivity contrasts.

[1] *CRC-AMET*
School of Earth and Planetary Sciences
Macquarie University,
NSW 2109
Phone: (02) 9850 9280
Facsimile: (02) 9850 8366
E-mail: David.Annetts@mq.edu.au

[2] *CRC-AMET*
School of Earth and Planetary Sciences
Macquarie University,
NSW 2109
Phone: (02) 9850 9280
Facsimile: (02) 9850 8366
E-mail: Fred.Sugeng@mq.edu.au

[3] *CRC-AMET*
School of Earth and Planetary Sciences
Macquarie University,
NSW 2109
Phone: (02) 9850 9280
Facsimile: (02) 9850 8366
E-mail: James.Macnae@mq.edu.au

[4] *CRC-AMET*
School of Earth and Planetary Sciences
Macquarie University,
NSW 2109
Phone: (02) 9850-9280
Facsimile: (02) 9850 8366
E-mail: Art.Raiche@mq.edu.au

INTRODUCTION

Airborne electromagnetic (AEM) surveys are excellent for mapping conductivity distributions over large areas. Interpreted data may be used to map salt scalds or as part of a mineral exploration programme. However, AEM data pose special challenges for interpretation, because typical surveys can easily accumulate over 2GB of data in as little as 3 hours (Lane et al., 1998).

In principle, one could invert the survey data as a whole for a multidimensional conductivity distribution, e.g., Alumbaugh and Newman (1998). However, formally inverting survey data for a 1D Earth is a formidable task that would take many months, and multidimensional inversion is considerably more difficult (Ellis, 1998). With this in mind, much effort has been invested in so-called 'rapid approximate' techniques. Variously called conductivity-depth imaging (CDI) or conductivity-depth transforms (CDT) in the literature, these were initially applied to ground EM data by Macnae and Lamontagne (1987) and Nekut (1987). The transformation of survey data to a conductivity-depth cross-section is based upon a receding image of the transmitter loop fitted to the response at each decay time. However, the transformation is approximate because the Earth is assumed to be 1D. Refinements of early CDI schemes are summarised by Wolfgram (1995).

It has long been known that interpretation of data collected over 3D and 2D geology using 1D methods can lead to erroneous interpretations (Scott and Fraser, 1973). Various schemes have been devised to minimise artefacts associated with 2D and 3D structures that lead directly to misinterpretation of data, e.g., Walker (1998), Zhdanov and Li (1998). However, despite their promise, such schemes are still very much in their infancy. Through study of the AEM response of several simple models, we sought an understanding of the artefacts associated with 2D structures and how these artefacts affect the response of genuine conductors.

NUMERICAL-MODELLING OF AEM DATA

We investigate the response of a 2D conductivity distribution excited by a 3D airborne source, the so-called 2.5D problem. This 2.5D problem, which was first studied by Stoyer and Greenfield (1976), allows quite realistic geology to be modelled easily. Although decay rates are slower than for 3D models (Sugeng et al., 1993), the 2.5D approximation is valid for models whose 2D sections are constant over strike lengths of 500 m or more.

We used the program Arjuna_Air (Sugeng and Raiche, 1997) for all models in this work. Using the frontal finite-element method (Sugeng et al., 1993), Arjuna_Air describes the Earth using 8-node isoparametric finite elements and solves the frequency-domain problem before transformation to the time domain using techniques described by Raiche (1998). The code's accuracy was tested by direct comparison with 1D solutions, e.g., Ward and Hohmann (1987), and we found good (<2%) agreement between solutions for models with resistivities between 0.01 and 1000 Ω.m when the measurement range was between 0.01 and 100 ms.

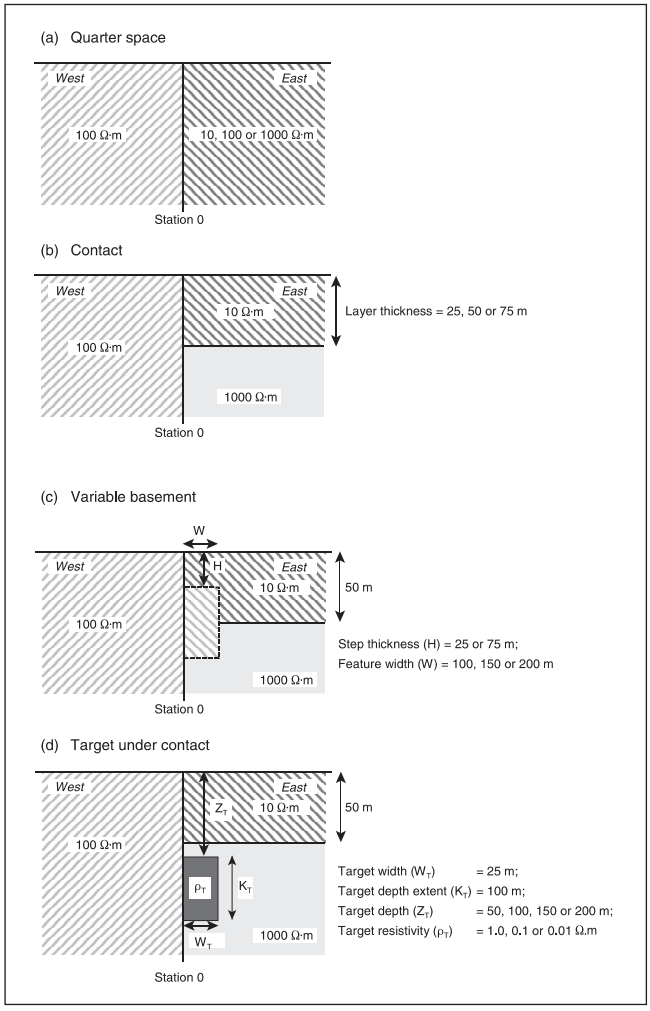

Fig. 1. Vertical contact models considered in this paper. A 100 Ω.m quarter-space was maintained in the western half of each model with parameter variation confined to the geo-electric section in the eastern half of each model.

VERTICAL-CONTACT MODELS

We consider four models containing vertical contacts as illustrated in Figure 1. All contacts have a north-south strike and the sections are plotted with east to the right. Figure 1a shows the first type of model; two quarter spaces. The western quarter space was maintained at 100 Ω.m while the eastern quarter space took values of 10, 100 and 1000 Ω.m. This range includes a 100 Ω.m halfspace. The boundary between the two quarter spaces was at Station 0. This family of models is referred to here as 'quarter-space models'. Quarter-space models were employed in the study of faults by Wilt (1991) and their theoretical response has been studied by Sampiao and Popov (1997).

The next vertical contact model we consider is the model illustrated in Figure 1b. As with quarter-space models we maintained a 100 Ω.m quarter space in the western part of the model, but in this case allowed layer thicknesses in the east of the model to vary. We consider three such 'contact models' where the thickness of the layer took values of 25, 50 and 75 m. We did not vary layer resistivities in the model's eastern half, maintaining them at 10 Ω.m for the upper layer and 1000 Ω.m for the basement.

The third type of model we consider, termed 'variable basement models', is illustrated in Figure 1c. Such models can be considered as two adjacent contact models and can be used to model regolith-dominated environments where conductance contrasts vary laterally as well as vertically. So as to permit comparison with contact models, we varied the thickness and width of a section of the 10 Ω.m resistivity near-surface layer in the model's eastern half. That part of the layer adjacent to the contact had a thickness of 25 or 75 m over a width of 100, 150 or 200 m. East of the variable section, the model consisted of a 50 m thick layer. The underlying basement had a resistivity of 1000 Ω.m. As before, we maintained a 100 Ω.m quarter space in the western part of the model.

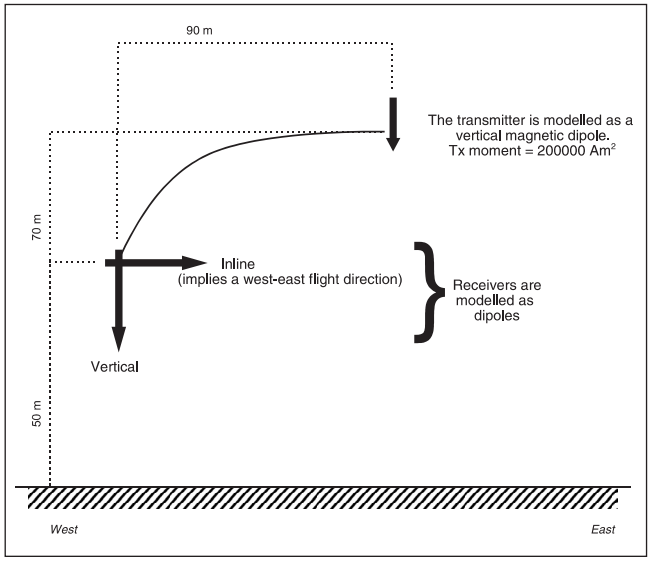

Fig. 2. Schematic of the prospecting system used in this paper. This system is similar to commonly-used fixed-wing prospecting systems.

The final model considered here is that of a 'target underlying a contact'. This is illustrated in Figure 1d. The target is 25 m wide, 100 m in depth extent and is at a depth of 50 m. We consider target-resistivities of 1, 0.1 and 0.01 Ω.m. With the exception of the target, the model is identical to a contact model (Figure 1b) with a 50 m thick 10 Ω.m resistivity layer overlying a basement with a resistivity of 1000 Ω.m.

We present data for a system that measures a magnetic field with a square-wave transmitter operating at a base frequency of 20 Hz. Although we computed model responses in 14 windows ranging from 0.01 ms to 17.78 ms, here, we restrict discussion to model responses at 0.01, 0.1, 1.0 and 10 ms. We modelled responses assuming a vertical dipole transmitter with a moment of 200×10^3 A.m^2, 120 m above the ground trailing a two-component dipole receiver 90 m behind and 70 m below. Our prospecting system has a similar configuration to the QUESTEM system described by Anderson et al. (1993) and is illustrated in Figure 2.

We plot data at the receiver coordinate and model responses for two flight directions. A west-east profile is defined as a flight left-right across the page, while an east-west profile is defined as a flight from right-left. Throughout this paper, west-east flight profiles are plotted as solid curves and east-west oriented flight profiles are plotted as dashed curves.

DISCUSSION

Quarter-space models

In Figure 3, we compare inline- and vertical-component responses computed for the various quarter-space models at 0.01, 0.1, 1.0 and 10.0 ms. It is immediately apparent that quarter-space

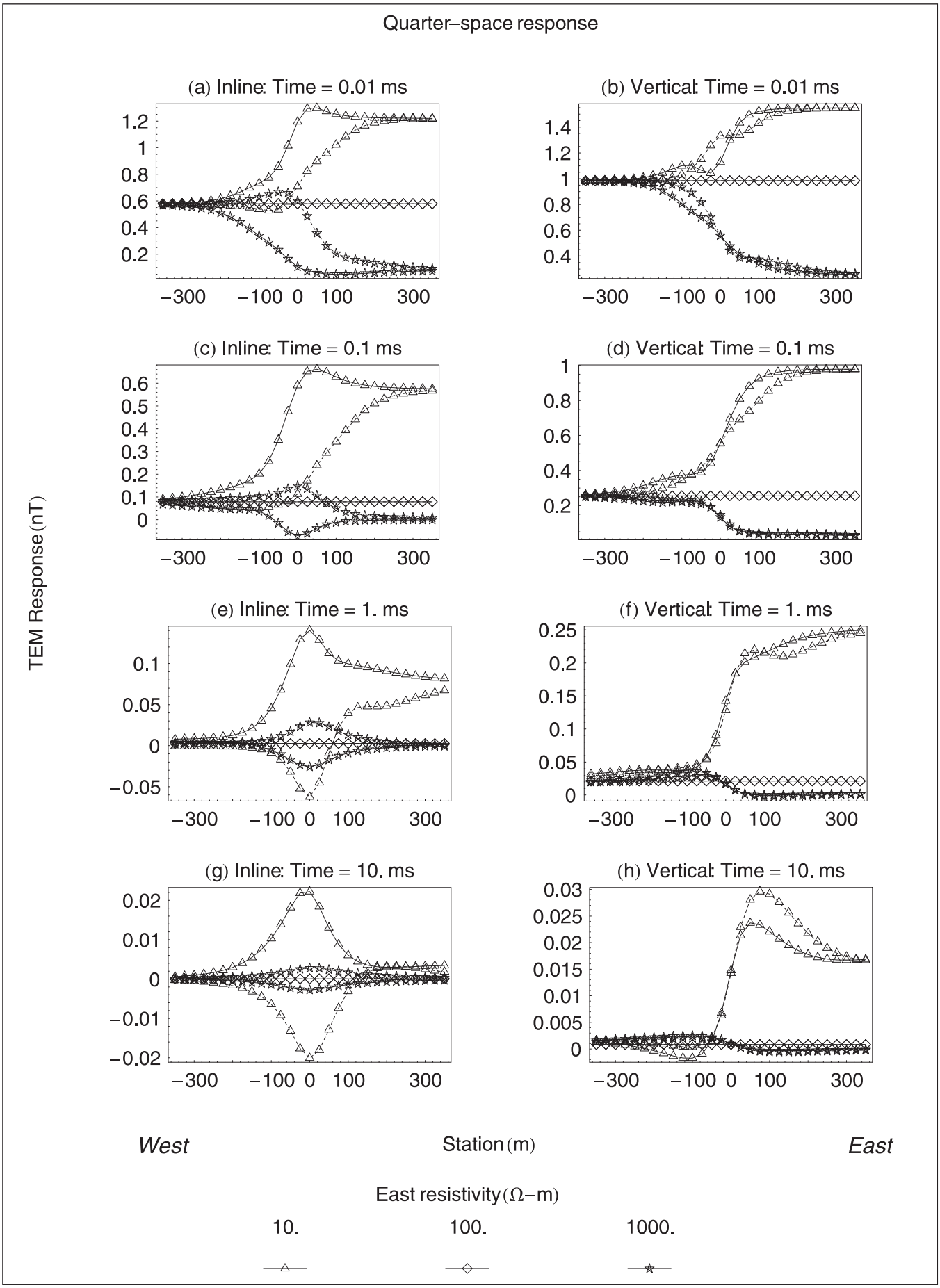

Fig. 3. Comparison of quarter-space model responses at 0.01, 0.1, 1.0 and 10.0 ms. Parameter variation is shown in Figure 1a. Dashed profiles were flown from east to west while solid profiles were flown from west to east.

responses have significant dependence on flight direction. This dependence causes a characteristic effect when data are plotted in map form and is commonly termed 'herring-boning'. The effect is generally stronger for inline-component data (Figures 3a, c, e, g) than for vertical-component data (Figures 3b, d, f and h). For inline-component data, flying from more resistive ground onto more conductive ground results in an overshoot in AEM response (relative to the normal response one would measure over a halfspace) in the vicinity of the boundary between the two quarter spaces. This increase in AEM response occurs up to 250 m either side of the actual boundary at 0.01 ms and increases with increasing time. For example, at 10.0 ms differences between quarter-space responses and their asymptotic halfspace responses are observed over 350 m either side of the boundary. When flying from conductive ground onto more resistive ground, the inline-component AEM response is reduced (again, relative to the normal response one would measure over a halfspace) in the vicinity of the boundary between the two quarter spaces. In contrast, vertical-component data tend to suffer overshoot on the more conductive side of the boundary independent of flight direction.

The significance of herring-boning is seen at later measurement times. Since currents tend to decay slowly in conductive media they tend to concentrate along the more conductive side of a boundary. This increases the response in the vicinity of the boundary, which persists at all measurement times following that at which the expanding smoke ring of current (Nabighian, 1979) reaches the boundary. Flying from resistive ground onto more conductive ground leads directly to a peak in the late-time inline-component response and also to a peak in the vertical-component response. Inline-component peaks are located closer to the boundary than vertical-component peaks. When flying from conductive ground onto more resistive ground, exactly the same situation occurs. However, inline-component data suffer a polarity reversal simply because the direction of current flow is reversed. Simple modelling of a steeply dipping thin plate in a resistive halfspace, e.g., Raiche (1997), shows that the response of a genuine conductor does not change polarity when the flight direction is reversed. The step AEM response of a vertical conductor is characterised by a single peak over the target for vertical-component data and by an asymmetric crossover for inline-

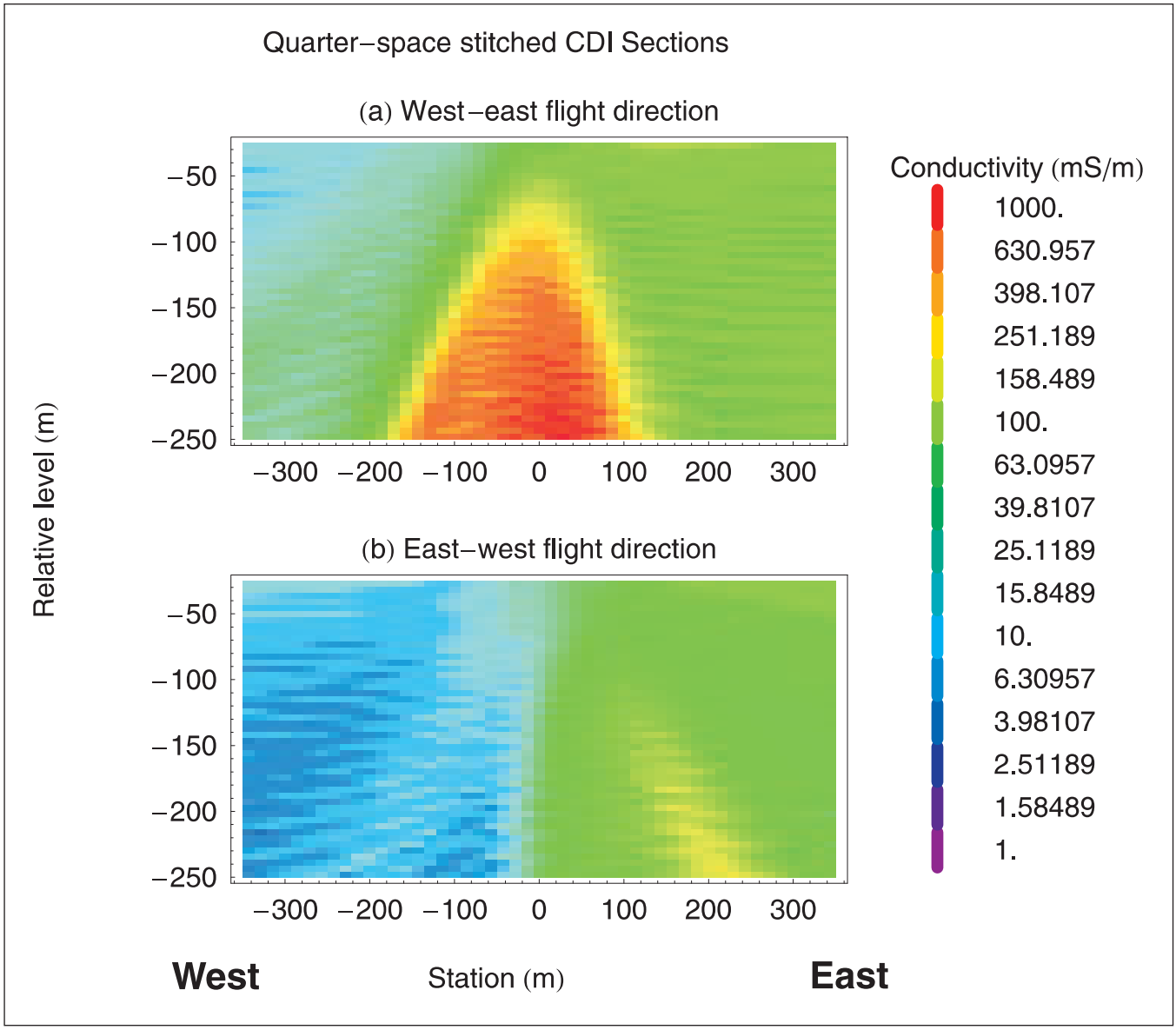

Fig. 4. Stitched CDI sections for 100 : 10 Ω.m quarter spaces. The contact between the spaces is at Station 0. In Figure 4a, the flight direction was from west to east and in Figure 4b, the flight direction was from east to west. Significant artefacts are apparent when flying from resistive ground in the west to more conductive ground in the east.

component data. However, because of background responses, the negative tail of the inline-component response may be absent. In this case, the response is characterised by a peak in both vertical- and inline-component responses.

The magnitude of the peak in late-time inline-component data, particularly for the model 100 Ω.m : 10 Ω.m in Figure 3g, is worthy of further comment. The amplitude of this peak is significantly greater than the background, and we suggest that in moderately noisy environments such an AEM response might warrant further investigation. Employing the rule-of-thumb that the depth to a conductor's top is given by the width of the anomaly at two-thirds its maximum amplitude (Gallagher et al., 1985), one would calculate a depth to conductor of 101 m based on data at 10.0 ms. If only inline-component data flown from west to east were available, we might consider further work on this potential target. Such an inclination would be confirmed when data were processed using a rapid interpretation technique such as the CDI process of Macnae et al. (1991), where this anomaly is imaged as a strong conductor. Figure 4 compares stitched CDI sections for a 100 : 10 Ω.m quarter-space model. In Figure 4a a strong artefact is evident at the boundary between the two quarter spaces where the system flies onto the more conductive space. Flying from the conductive section to the resistive section (Figure 4b), the artefact is resistive, and its spatial extent is considerably reduced.

Contact models

Figure 5 compares inline- and vertical-component responses computed for the various contact models at 0.01, 0.1, 1.0 and 10 ms. As expected from modelling layered Earths, differences between the three different contact responses are first observed at 0.1 ms (Figures 5c and d), where the response of the 25 m thick contact can be distinguished from its thicker counterparts. By 1.0 ms (Figures 5e and f), it is possible to differentiate the response of all three models. As with the quarter-space responses illustrated in Figure 3g, contact-model responses at 10.0 ms in Figure 5 show peaks in inline-component data near Station 0, with polarity reversals when the flight direction is towards the more resistive west.

Late-time vertical-component contact model data differ from later time quarter-space model data slightly. The tendency for quarter-space responses is to asymptote (spatially) to the response of an equivalent half-space. For late-time responses, this means that although there is a peak in the response because of the boundary, the response is greater on the more conductive side of the profile. For our contact model we must note that although the section west of Station 0 is more resistive than the top 25 m of the section east of Station 0, the basement east of Station 0 is more resistive than the basement west of Station 0. For thin contacts, this means that the peak in vertical-component data observed at late times migrates towards the more conductive part of the section. This is observed in Figure 5h where peak AEM responses from the 25 m thick contact model are closer to Station 0 than those from the other two models.

Variable-basement models

The first variable-basement model is that with the 25 m thick contact that thickens to 50 m at distances of 100, 150 or 200 m from Station 0. AEM responses from the various forms of this model are compared in Figure 6. The second variable-basement model has a 75 m thick contact that decreases in thickness to 50 m, again at distances of 100, 150 or 200 m from Station 0. AEM model responses from this type of model are compared in Figure 7.

As with contact-model responses, variable-basement model responses are very similar to the response of a 100 Ω.m : 10 Ω.m quarter-space at very early times. Differences between the models are first observed in Figures 6c and d where the EM fields have penetrated the 25 m thick section. At 0.1 ms (Figure 6c), we note that the inline-component AEM response for shorter features has greater magnitude than the AEM response of longer ones. For west to east profiles, these differences are most apparent between Stations 0 and 150. For east to west profiles, differences are most apparent between Stations 100 and 300. At Station 300, the transmitter of our east to west flying system is closer to the 25 m thick section of the 200 m long feature so the response of this model has lower magnitude than the other two. Similarly, near Station 250 the transmitter is closer to the 25 m thick section than to the 50 m thick section and the response of the 150 m long feature has lower magnitude than the response of the 100 m long feature. At Station 100, responses from each model converge because the underlying geo-electric section is identical for each model. For vertical-component data (Figure 6d), differences between model responses appear largely independent of flight direction and are observed between Stations 50 and 250.

At 1.0 ms differences in the responses of all models are observed. In Figure 6e inline-component data have peaks corresponding directly to changes in the structure of the model. For models flown east to west, these peaks are negative. At 1.0 ms the highest amplitude responses are observed for models containing wider features. However, models with 100 m wide features have higher amplitude responses at Station 0. For vertical-component data (Figure 6f), the major differences between model responses are observed between Stations 100 and 200. In this region, as with inline-component data, higher amplitude responses are associated with shorter features. Since vertical-component data converge to background responses more quickly than their inline counterparts, we suggest that the most accurate mapping of subsurface conductance contrasts might be achieved using vertical-component data only.

At later delay times, the relative magnitude of inline-component response peaks changes again. At 10.0 ms (Figure 6g), maximum amplitude for all model responses is found at Station 0 at the quarter-space boundary. Smaller peaks are observed, and these correspond with changes in the thickness of the surface layer. For vertical-component data (Figure 6h), changes in the layer's thickness are associated with inflexion points. For late-time data, it is generally the case that shorter features have larger responses than longer ones. This is because the effects from edges in closer proximity are superimposed.

Data in Figure 7 were computed for the second variable basement model in which layer thickness is reduced from 75 m to 50 m at distances of 100, 150 and 200 m from Station 0. The differences between the computed responses of this set of models are less profound than those in Figure 6. Since there is a thicker conductive section in these models, differences in model responses are clearer at times later than 0.1 ms. In Figures 7e and f wider features generally have larger responses than narrower ones. These differences persist at later times. For the inline-component data in Figure 7g, changes in model thickness are associated with response extrema. For example, for west to east flown inline-component profiles, the response maximum occurs at the quarter-space boundary at Station 0. Minima within the profiles occur near the next change in the thickness of the surface layer. East to west flown profiles have anomalies that are reversed in polarity. Inflexion points in the eastern portion of the vertical-component profiles in Figure 7h correspond with changes in the surface layer's thickness.

Our final comment on variable-basement model responses relates to profile shape. All model responses, in particular models with a step from 75 m to 50 m, contain significant peaks at late times similar to the signature of a genuine bedrock conductor. For

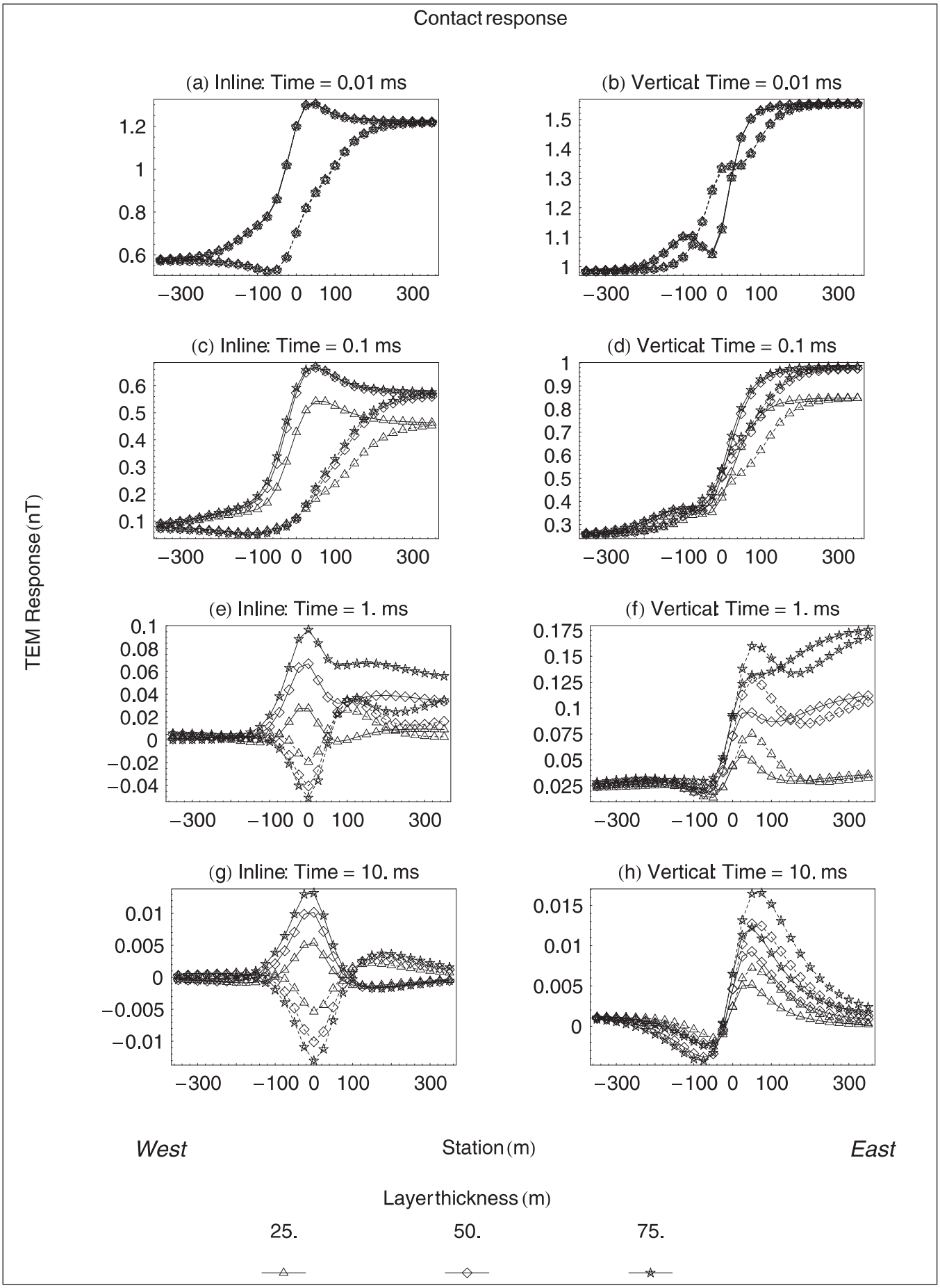

Fig. 5. Comparison of contact model responses at 0.01, 0.1, 1.0 and 10.0 ms. Parameter variation is shown in Figure 1b. Dashed profiles were flown from east to west while solid profiles were flown from west to east.

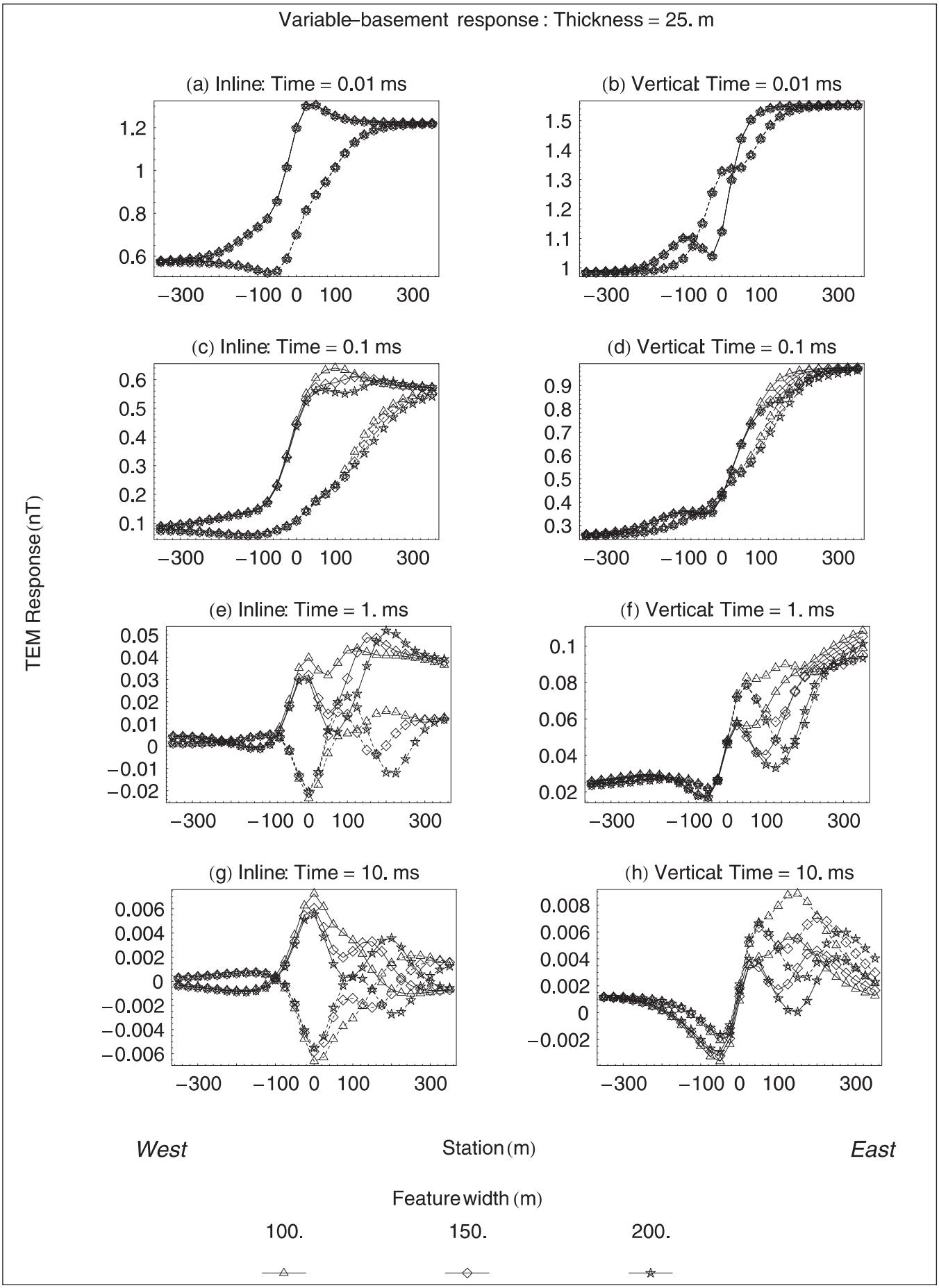

Fig. 6. Comparison of variable-basement model responses for 25 to 50 m steps at 0.01, 0.1, 1.0 and 10.0 ms. Parameter variation is shown Figure 1c. Dashed profiles were flown from east to west while solid profiles were flown from west to east.

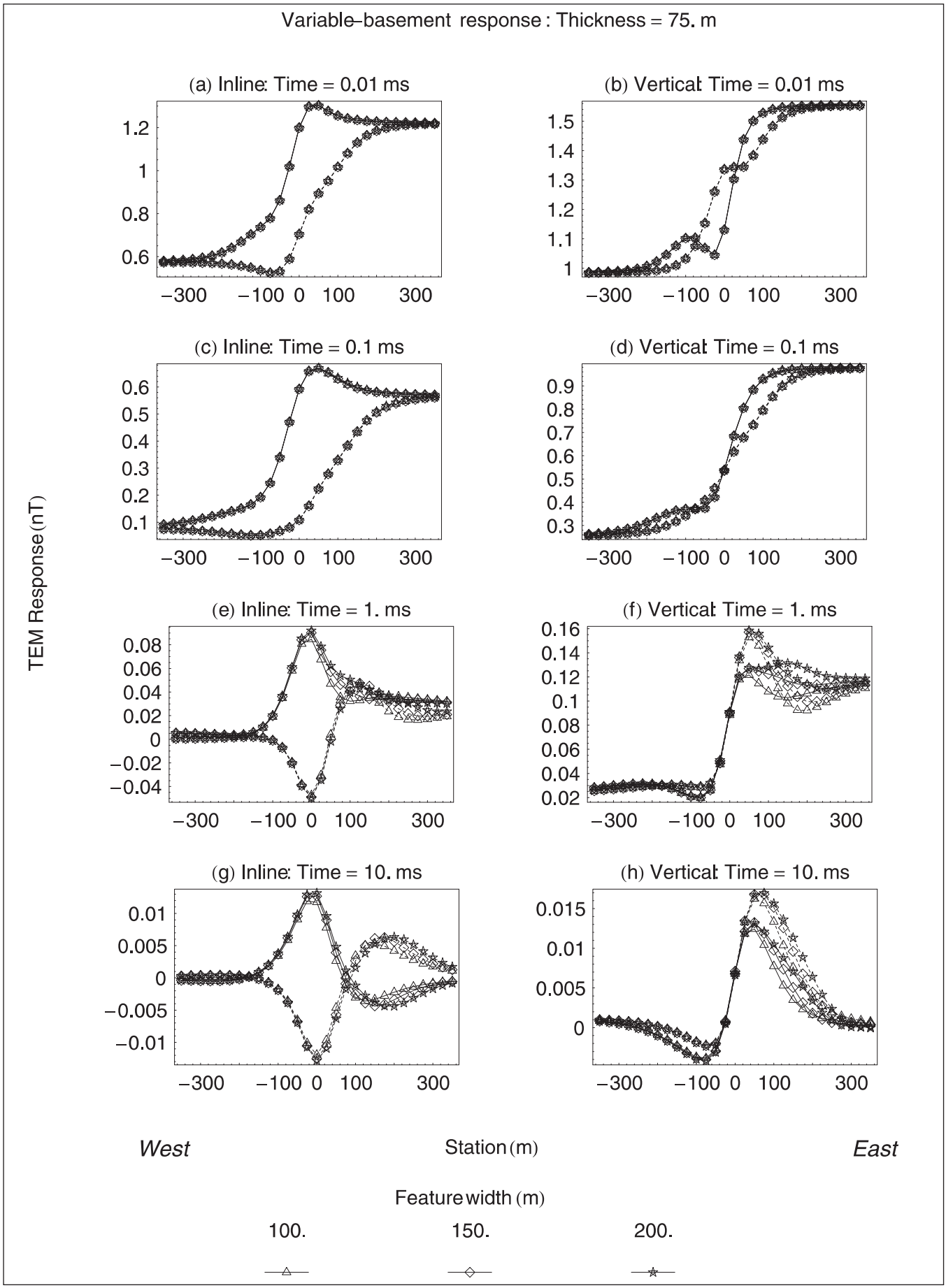

Fig. 7. Comparison of variable-basement model responses for 75 to 50 m steps at 0.01, 0.1, 1.0 and 10.0 ms. Parameter variation is shown in Figure 1c. Dashed profiles were flown from east to west while solid profiles were flown from west to east.

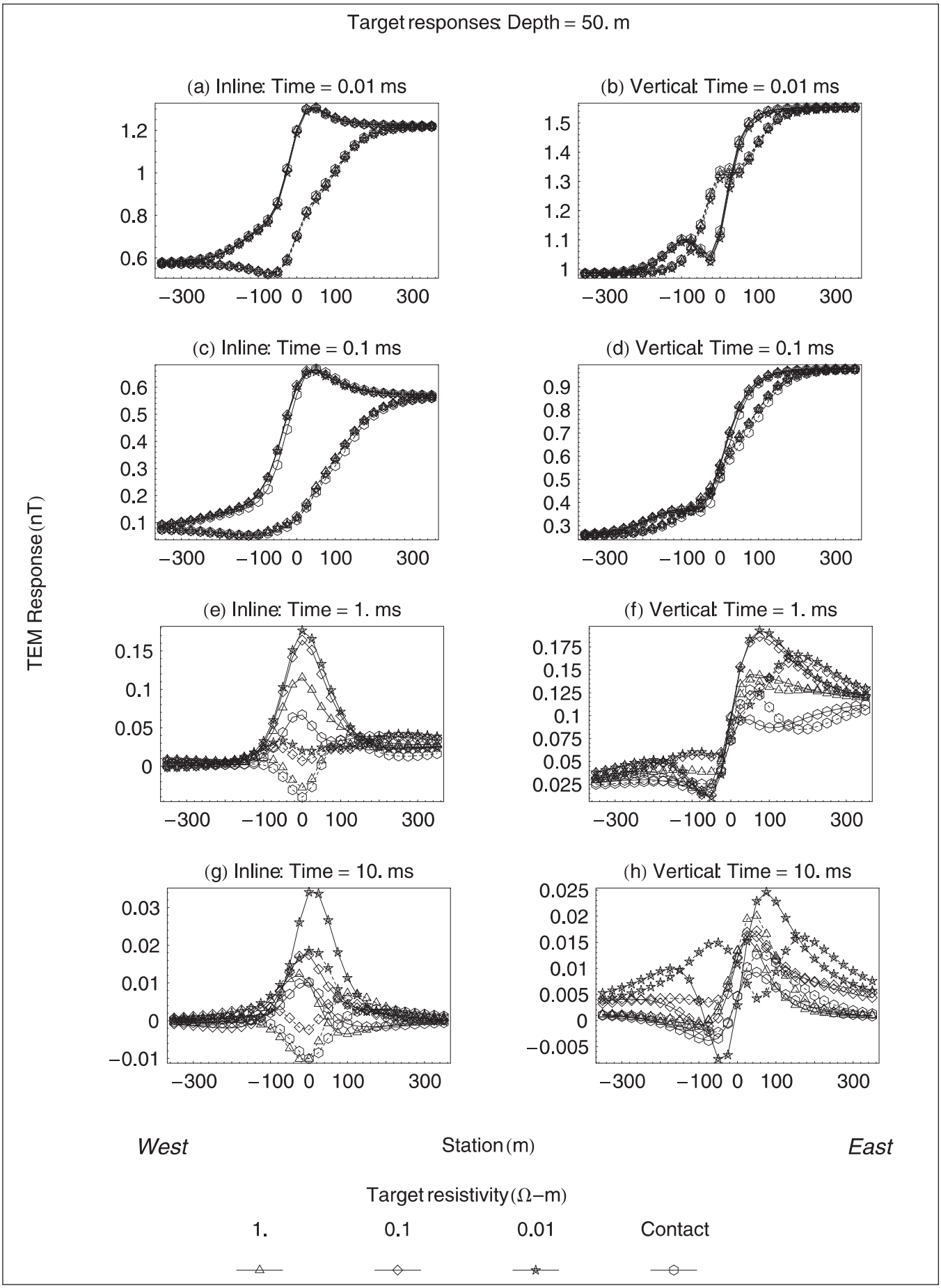

Fig. 8. Comparison of target model results with 50 m thick contact model results at 0.01, 0.1, 1.0 and 10.0 ms for a target with a depth-to-top of 50 m. Parameter variation is shown in Figure 1d. Dashed profiles were flown from east to west while solid profiles were flown from west to east.

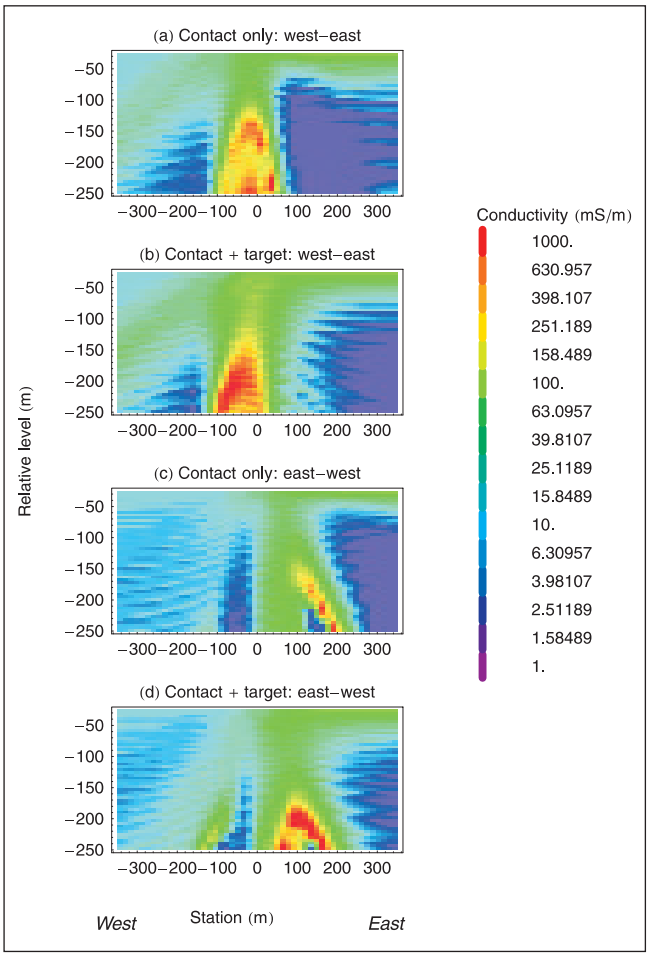

Fig. 9. Comparison of stitched CDI sections for contact and 1 Ω.m target at a depth of 50 m lying directly beneath a 50 m thick contact. The lateral extent of the target is from Station 0 to 25. Figures 9a and 9b compare sections for west to east profiles of contact and target models, while Figures 9c and 9d compare profiles for east to west contact and target models. The target is largely obscured by artefacts when flying from the resistive west to the more conductive east.

east to west flown profiles, rules-of-thumb for conductor depths would place bedrock conductors at depths of 102, 116 or 131 m for vertical-component data, and at depths of 108, 113 and 129 m for inline-component data.

Target underlying contact model

Figure 8 compares the response of a contact with that of a target directly underlying a contact for targets with resistivities of 1.0, 0.1 and 0.01 Ω.m. Inclusion of a target has influenced the response at times later than 0.1 ms (Figures 8c and d), but the nature of this influence differs depending on flight direction and target resistivity. When the flight direction is from west to east the responses from the target and the contact are superimposed, increasing anomaly amplitudes but with little effect on anomaly shape. However, when the flight direction is from east to west, the superposition of the responses from the target and the contact affects the shape of the anomaly markedly, depending upon target resistivity. This is most easily seen in Figure 8g. The inline-component response is a trough directly over the target when the target has a resistivity of 1 Ω.m. However, when target resistivity is 0.01 Ω.m, the inline-component response is a peak directly over the target. The effect of profile direction on the vertical-component data is most clearly seen in Figure 8f, where the effect of the target on east-west oriented profiles is to change the location of the anomaly's peak from Station 75 to Station 150.

An example of the use of herring-boning to detect a bedrock conductor is given in Figure 9. Figure 9 compares stitched CDI sections from 50 m thick contact models and a model of a 1 Ω.m target directly under a 50 m thick contact. Sections with west-east flight directions (Figures 9a and b), look fairly similar, and the presence of the conductor is only apparent from slightly higher conductivity values between Stations -100 and -50. Sections with east-west flight directions (Figures 9c and d) are also very similar in terms of their artefacts. A conductive zone between Stations 50 and 100 betrays the presence of the target. When the flight direction is reversed, the character of artefacts in these stitched CDI sections changes, but the character of genuine conductors does not.

CONCLUSIONS

We have modelled the fixed-wing AEM response of a number of vertical contact models. We found that quarter-space models were very good predictors of the response of vertical contacts at very early times, but that as measurements were made at later times, more complex responses were observed. To this end, we recommend the use of models that reflect the underlying geology at all stages of interpretation.

We found that the AEM response of all our models of vertical contacts possessed artefacts at later measurement times and that, relative to a background response, the magnitude of these artefacts increased with later measurement times. Profiles of later-time data were suggestive of the response of deep plate-like conductors. When genuine deep conductors were included in contact models we found that the response of the artefact associated with the vertical-contact was sufficient to overwhelm the response of the genuine deep conductor.

We found that late-time artefacts could be resolved only by using response offsets that may appear as herring-bone effects in multiple-component, broadband AEM measurements. This implies that closely spaced lines flown in opposite directions may be needed for accurate interpretation. Our results show that worst-case AEM surveys are single-line and 'racetrack-mode' inline-component surveys. Such surveys permit detection of anomalies associated with conductivity contrasts. However, one can not determine whether such anomalies are caused by near-surface or deeper conductivity contrasts because there are inadequate data.

ACKNOWLEDGEMENTS

This work was performed under the auspices of the Australian Government's Cooperative Research Centres Program. It was partially funded by the sponsors of AMIRA Project P223C: Aberfoyle Resources, BHP Minerals, CRA Exploration, M.I.M. Exploration, North Pasminco Exploration, PNC Exploration (Australia), Sumitomo Metal Mining Oceania, Cominco Exploration, Anglovaal, and Gencor. We thank sponsors of AMIRA Project P407 for use of the software package EMFlow, and for the input of geological parameters contributing to more realistic numerical models. We are also grateful for the insight into this topic gained through conversations with J. Chen, J. Reid and B. R. Spies, all of the CRC-AMET. DA additionally acknowledges a CRC-AMET scholarship. This paper is published with the encouragement of the director of the CRC-AMET.

REFERENCES

Alumbaugh, D.L. and Newman, G.A., 1997, Three-dimensional massively parallel electromagnetic inversion - II. Analysis of a crosswell electromagnetic experiment: Geophys. J. Internat., 128, 355-363.

Anderson, H.F., Duncan, A.C. and Lynch, S.M., 1993, Geological mapping capabilities of the QUESTEM airborne electromagnetic system for mineral exploration - Mt Isa Inlier, Queensland: Expl. Geophys., 24, 333-340.

Ellis, R.G., 1998, Inversion of airborne electromagnetic data: 68th Ann. Internat. Mtg. Soc. Expl. Geophys., Expanded Abstracts, 2017-2019.

Gallagher, P.R., Ward, S.H. and Hohmann, G.W., 1985, A model study of a thin plate in free space for the EM37 transient electromagnetic system: Geophysics, 50, 1022-1019.

Lane, R., Plunkett, C., Price, A., Green, A. and Hu, Y., 1998, Streamed data - A source of insight and improvement for time domain airborne EM: Expl. Geophys., 29, 16-23.

Macnae, J.C. and Lamontagne, Y., 1987, Imaging quasi-layered conductive structures by simple processing of transient electromagnetic data: Geophysics, 52, 545-554.

Macnae, J.C., Smith, R., Polzer, B.D., Lamontagne, Y. and Klinkert, P.S., 1991, Conductivity-depth imaging of airborne electromagnetic step-response data: Geophysics, 56, 102-115.

Nabighian, M.N., 1979, Quasi-static transient response of a conducting half-space - an approximate representation: Geophysics, 44, 1700-1705.

Nekut, A.G., 1987, Direct inversion of time-domain electromagnetic data (short note): Geophysics, 52, 1431-1435.

Raiche, A., 1997, Leroi_Air, Modelling program developed for the sponsors of Australian Minerals Industries Research Association Project, P223C.

Raiche, A., 1998, Modelling the time-domain response of AEM systems: Expl. Geophys., 29, 103-106.

Sampaio, E.E.S. and Popov, M.M., 1997, Zero-order time domain scattering of electromagnetic plane waves by two quarter spaces: Radio Sci., 32, 305-315.

Scott, W.J. and Fraser, D.C., 1973, Drilling of EM anomalies caused by overburden: CIM Bull., July, 72-77.

Stoyer, C.H. and Greenfield, R.L., 1976, Numerical solutions of the response of a two-dimensional earth to an oscillating magnetic dipole source: Geophysics, 41, 519-530.

Sugeng, F. and Raiche, A., 1997, Arjuna_Air, Modelling program developed for the sponsors of Australian Minerals Industries Research Association Project, P223C.

Sugeng, F., Raiche, A. and Rijo, L., 1993, Comparing the time-domain EM response of 2-D and elongated 3-D conductors excited by a rectangular loop source: J. Geomag. and Geoelec., 45, 873-885.

Walker, P. 1998, A new AEM imaging algorithm for use in conductive areas: Expl. Geophys., 29, 184-190.

Ward, S, and Hohmann, G.W., 1987, Electromagnetic theory for geophysical applications, in Nabighian, M.N., Ed., Electromagnetic methods in applied geophysics volume 1: (Theory): Soc. Expl. Geophys., 130-311.

Wilt, M.J., 1991, Interpretation of time domain electromagnetic soundings near geological contacts: Ph.D thesis, Univ. of California.

Wolfgram, P., 1995, Discussion on: "Conductivity-depth transform of GEOTEM data": Expl. Geophys., 26, 549.

Zhdanov, M.S. and Li, W. 1998, Preconditioned time domain electromagnetic migration: 68th Ann. Internat. Mtg. Soc. Expl. Geophys Expanded Abstracts, 461-464.